RSC Advances

PAPER

View Article Online
View Journal | View Issue

Cite this: *RSC Adv.*, 2022, **12**, 33358

Photo-controlled and photo-calibrated nanoparticle enabled nitric oxide release for anti-bacterial and anti-biofilm applications†

Li Li,‡[a] Zhenmei Lin,‡[a] Xicun Lu,[b] Chen Chen,[a] Anqi Xie,[a] Yaoping Tang[a] and Ziqian Zhang *[a]

Received 26th August 2022
Accepted 11th November 2022

DOI: 10.1039/d2ra05352g

rsc.li/rsc-advances

After numerous efforts to elucidate the biological role of nitric oxide (NO), NO treatments have become a hotspot at the forefront of medicine. NO-releasing substances are constantly needed, while the direct use of NO gas is unattainable in bio-systems. An ideal NO donor should possess controllable and visible NO-release capability. The reported NO donating nanoparticles, prepared *via* encapsulating a hydrophobic NO-releasing compound into DSPE-PEG_{2000}, meet the criteria mentioned previously. The localization and flux of NO released from these nanoparticles could be manipulated by UV or blue light. Meanwhile, NOD-NPs emit a dose-dependent fluorescence intensity to calibrate the generation of NO. While the good biocompatibility of NOD-NPs has been validated, the NO from our nanoparticles demonstrates efficient anti-bacterial and anti-biofilm effects toward *Escherichia coli* (*E. coli*) and *Staphylococcus aureus* (*S. aureus*). Therefore, the NOD-NPs developed in this work have potential application in evaluating the regulation of microbes by NO.

Introduction

It is acknowledged that nitric oxide (NO) donors have been used for disease treatments for a long time.[1,2] In the nineteenth century, glyceryl trinitrate (GTN) was adopted to relieve cardiovascular diseases, such as angina pectoris. But no one realized that the efficacy was due to NO released from GTN until the 1980s.[3–6] Since then, extensive studies have demonstrated that NO plays a crucial role in various physiological and pathological processes, including vasodilation, cellular proliferation, neurotransmission, inflammation, and infection.[7–11] Recently, Boon *et al.* reported that the formation of bacterial biofilms is also regulated by NO.[12] The reports concluded that a low concentration of NO would trigger biofilm dispersal, and NO at a high concentration would directly kill the bacteria. While the concentration of NO is a pivotal factor in the therapeutic effect, precise control and calibration of NO-release by NO donors are urgently needed. Nevertheless, the gold standard NO donors, such as sodium nitroprusside, organic nitrates, and NONOates, spontaneously release NO.[13–15] And their kinetics, localization, and dose of NO released are heavily manipulated by the biological environment, for example, enzymes, thiols, and pH.[15] Without additional NO analysis methods, essential information on NO-release is absent. Some analytical approaches for NO would damage bio-samples, hence the analysis results lack timeliness.[16,17] Fluorescent probes could monitor NO in real-time and are friendly to the samples, but they are not appropriate for measuring NO from donors, because detection is achieved by exhausting NO and invalidating the biological outcomes of the NO donor.[18–21] Based on the above, a photo-triggered NO donor would be a solution for dynamic and localized NO-release, while a photo-calibrated donor enables real-time quantification of the dose of NO.

To date, numerous achievements in developing functional NO donors have been made.[22–29] Among these advances, *N*-nitrosated push–pull dyes, which are further designed to be photo-controllable and photo-measurable, are probably ideal NO donors.[30–33] The *N*-nitrosamine dye would be photo-decomposed into NO and the corresponding fluorescent dye. First, light could spatiotemporally control the flux of NO-release by amplifying or attenuating the photo intensity. Second, the NO release could be monitored in real-time and calibrated using the fluorescence emitted by the dye.

The co-polymer DSPE-PEG_{2000} (1,2-distearoyl-*sn*-glycero-3-phosphoethanolamine-*N*-[methoxy-(polyethylene glycol)-2000]) and its derivative, which mostly facilitates the solubility of hydrophobic substances, improves the bioavailability of drugs, reduces biotoxicity, and acts as a targeting carrier, have been

[a]*Guangxi Scientific Research Center of Traditional Chinese Medicine, Guangxi University of Chinese Medicine, Nanning 530200, China. E-mail: jxiaozzq@hotmail.com*

[b]*State Key Laboratory of Bioreactor Engineering, Shanghai Key Laboratory of Chemical Biology, School of Pharmacy, East China University of Science and Technology, Shanghai 200237, China*

† Electronic supplementary information (ESI) available. See DOI: https://doi.org/10.1039/d2ra05352g

‡ These authors contributed equally to this work.

widely employed in the preparation of advanced nanoparticles.[34–37]

Herein, an *N*-nitrosated naphthalimide (NOD-C18) tethered to a long alkyl chain was acquired, and the NOD-C18 would be triggered by UV light to generate NO and the fluorescent dye Nap-C18 (Fig. 1a). The NOD-C18 was efficiently encapsulated into hydrophilic nanoparticles (NOD-NPs) with DSPE-PEG_{2000}. When exposed to 365 nm or 450 nm light, the NOD-NPs contributed to the highly spatiotemporal release of NO in solution or RAW264.7 cells (Fig. 1b). An excellent linear relationship between NOD-NPs' fluorescence intensity and the dose of NO was established, called photo-calibration. The nanoparticles exhibit good biocompatibility and low cytotoxicity. When the NOD-NPs were applied to deal with *E. coli* and *S. aureus*, the apparent antibacterial effect was due to the immediate release of NO. The regulation of bacterial biofilms was also demonstrated (Fig. 1c).

Results and discussion

We have synthesized NOD-C18 *via* a four-step reaction, and the relevant details are shown in Fig. S1.† The structural characterization, such as ^{1}H-NMR, ^{13}C-NMR, and MS data, is provided in the ESI (Fig. S10–S15†). With the molecule in hand, we tried to test its fluorescent properties under UV irradiation in tetrahydrofuran (THF). The NOD-C18 exhibited non-fluorescence in the polar solvent. Dramatically enhanced fluorescence emerged at 510 nm, which indicated that Nap-C18 was generated (Fig. S2†). In previous reports, fluorophore-based nitrosamine compounds were utilized for real-time monitoring and calibration of the NO-release in an aqueous or bio-system.[38,39] Therefore, we believe that NO was released spontaneously when the NOD-C18 transformed into Nap-C18. Then, the fluorescent properties of Nap-C18 were studied in different water fractions (Fig. S2†). The fluorescence intensity of Nap-C18 gradually decreased to non-fluorescence when the water fraction was increased from 0% to 100%. These results are due to the long aliphatic chain attached to the naphthalimide, which induced the aggregation-caused quenching (ACQ) effect in high polarity solvent. However, the long lipophilic alkyl chain was purposefully designed to maintain the free intramolecular motion of NOD-C18 inside some amphiphilic polymers. Accordingly, the fluorogenic product of NOD-C18 would show a quantitative relationship between fluorescence intensity and concentration for further application.

To improve biocompatibility and ensure good water dispersibility, NO donor nanoparticles (NOD-NPs) were prepared by directly encapsulating NOD-C18 into the amphiphilic copolymer DSPE-PEG_{2000} (Fig. 2a). The DSPE-PEG would form a rounded surface layer, and the hydrophobic NOD-C18 would be retained in the core of the spherical nanoparticle. The rational ratio between NOD-C18 and DSPE-PEG was confirmed by fluorescence spectroscopy of Nap-C18 encapsulated by DSPE-PEG (Fig. S3†). 0.5–25 μg mL^{-1} Nap-C18 was encapsulated into nanoparticles with 0.2 mg mL^{-1} DSPE-PEG, and the fluorescence intensity was further recorded. As shown by the data, fluorescence intensity linearly increases from 4 to 10 μg mL^{-1} Nap-C18. Next, we utilized 10 μg mL^{-1} Nap-C18 to afford NPs with different concentrations of DSPE-PEG (0.02–0.2 mg mL^{-1}). As shown in Fig. S3d,† the fluorescence intensity of NPs was gradually enhanced to a plateau at 0.08 mg mL^{-1} DSPE-PEG. Thus, the final conditions for NOD-NP construction were 1 mg NOD-C18 in 1 mL THF encapsulated by 8 mg DSPE-PEG in 9 mL water. After sonication and removing the THF by violent stirring, different concentrations of NOD-NP solution were obtained by dilution or condensation. We calculated the average encapsulation efficiency of the optimized product as 81.36 ± 1.7% according to the absorption at 350 nm of each batch of NOD-C18 supernatant (Fig. S4†). We anticipated that the NOD-NPs afforded with this particular ratio would enable fluorescence self-calibration.

Dynamic light scattering (DLS) measurement was utilized to characterize the NOD-NPs. The obtained nanoparticles possess an average hydrodynamic diameter of around 190 nm and a Zeta potential of −22.2 mV. And the transmission electron microscopy (TEM) observation shows that NOD-NPs form a uniform spherical morphology and the micelles have an average size of around 166.5 nm in diameter (Fig. 2b). Next, we kept the NOD-NPs in aqueous solution for 72 hours and the stability of the nanoparticles was also confirmed by TEM and DLS (Fig. S6†). After preparation for 24, 36, and 72 hours, the TEM images indicated that the diameters of NOD-NPs were still

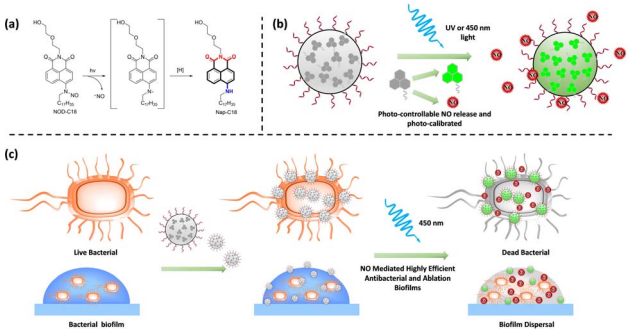

Fig. 1 (a) The mechanism of NOD-C18 degradation upon exposure to irradiation. (b) Illustration of an NOD-NP triggered by light to release NO. (c) Schematic illustration of the anti-bacterial and anti-biofilm activity of NO released from NOD-NPs.

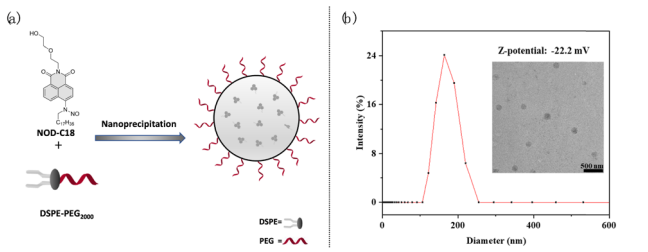

Fig. 2 (a) Illustration of NOD-NP formation by nanoprecipitation; (b) the DLS, Zeta potential and TEM results of NOD-NPs. Scale bar: 500 nm.

around 160 nm (Fig. S6A†). And the DLS measurements showed that the average diameter was in the range of 160–180 nm (Fig. S6B†). We could affirm that the shape and size of the nanoparticles changed inappreciably during this period of time. The corresponding Zeta potential was still maintained at around −22 mV (Fig. S6C†). All the results showed that NOD-NPs are rather stable in aqueous solution.

Subsequently, we evaluated the photophysical properties of NOD-NPs. Under irradiation with 365 nm UV light (40 mW cm^{-2}), the UV-vis absorption and fluorescence emission spectra of NOD-NPs (0.08 mg mL^{-1}) in 40 mM PBS solution changed rapidly (Fig. 3a). The maximum absorption peak of NOD-NPs at 355 nm gradually decreased, and a new absorption peak at 450 nm increased concurrently. Meanwhile remarkable enhancement of the green fluorescence signal ($\lambda_{ex} = 450$ nm) at 545 nm occurred.

After comparing UV-vis spectra of NOD-C18 and NOD-NPs, we found that NOD-NPs presented a broader absorption peak than NOD-C18 did (Fig. S7†). Hence, we supposed that NOD-NPs could be activated by blue light. To confirm our assumption, a NOD-NP buffer solution was directly exposed to blue light (40 mW cm^{-2} at 450 nm), which led to similar spectral changes to UV irradiation (Fig. 3b). Under the same intensity of irradiation light, UV light led to a thorough decomposition of NOD-NPs in about 120 seconds. Meanwhile the same decomposition triggered by blue light was completed in 1500 seconds (Fig. 3c). These phenomena were consistent with the UV-vis experiment in which NOD-NPs presented weaker absorption at 450 nm than at 365 nm. In bio-systems, visible light is much more biocompatible than UV light. Moreover, irradiation with different wavelengths could be a convenient approach to manipulating the dynamics of NO release. We used the reference dye rhodamine 6G ($\Phi_f = 0.95$ in ethanol) to determine the fluorescence quantum yield of the photolysis product ($\Phi_f = 0.27$).

Spatially-controlled and dose-controlled NO release has a critical influence on the therapeutic effects of NO. In our design, light switches on NO-release, and a turn-on fluorescent signal is accompanied by NO generation. Therefore, we attempted to localize and quantitate the NO release by a fluorimetric method. Firstly, we verified the generation of NO using the commercial fluorescent probe 2,3-diaminonaphthalene (DAN).[40] As shown in Fig. 3d, UV and blue light irradiation both caused the donor to release NO to a final dose. And the dynamics of NO release exhibit a similar trend to the fluorescence kinetics of NOD-NPs. These results indicated that the accompanying fluorescence of NOD-NPs could be used for monitoring NO release. Moreover, rate-control of our NO donor is achieved using different wavelengths of light. Hence, our nanoparticles provide a convenient approach to releasing and localizing NO. Secondly, the Griess assay was also employed to quantify the NO-release of NOD-NPs (0.01–0.1 mg mL^{-1}).[41] After exposure to blue light for 60 min, the total amount of NO released by NOD-NPs was measured by Griess assay. Then, we established an excellent linear curve ($R^2 = 0.9997$) between the concentration of NOD-NPs and the dose of NO (Fig. S8a†). We also recorded the fluorescence intensity of different concentrations of NOD-NPs, and plotted a perfectly linear curve (Fig.-S8b†). Based on these curves, we can harness the fluorescence intensity of NOD-NPs to calibrate the NO-release, since the intensity is proportional to the concentration (Fig. S8c†). According to previous reports, some NO-releasing nanoparticles were endowed with photo-monitoring functions, but few possessed the ability of photo-calibrated NO release.[42,43] Importantly, utilizing the obtained nanoparticles, the NO release could be followed over time.

The controllable NO-release was further investigated in a macrophage cell line. The NOD-NPs and dihydrochloride (DAPI) were co-incubated with RAW 264.7 cells for 30 min. After being washed three times, the treated cells were imaged using a confocal laser microscope. Only blue fluorescence emitted by DAPI was detected in the dark, implying that NOD-NPs were not activated to release NO. Then, the appearance of significant green fluorescence followed one-second of irradiation with 365 nm UV light. However, for an irradiation time of 10 s, the

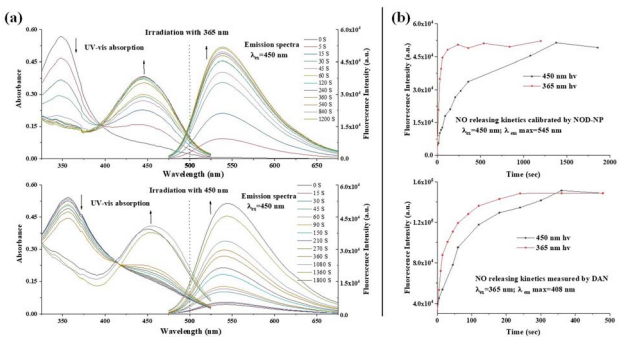

Fig. 3 (a) The time-dependent UV-vis absorption and fluorescence ($\lambda_{ex} = 450$ nm) spectra of NOD-NPs (0.08 mg mL^{-1}) irradiated with 365 nm light; (b) the time-dependent UV-vis absorption and fluorescence ($\lambda_{ex} = 450$ nm) spectra of NOD-NPs irradiated with 450 nm light; (c) fluorescence dynamics of NOD-NPs irradiated with 365 nm and 450 nm light; (d) the dynamics of NO release measured using DAN.

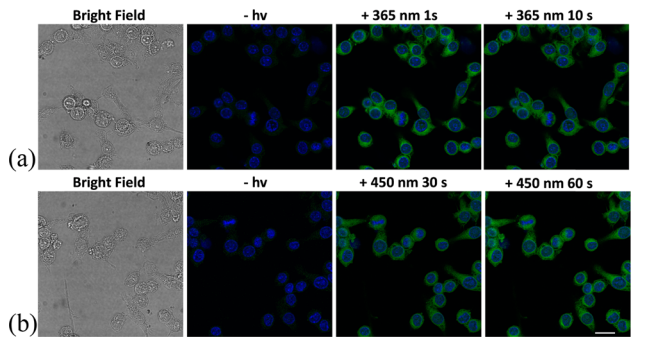

Fig. 4 The fluorescence images of RAW 264.7 cells captured using a confocal laser scanning microscope. (a) The cells were treated with DAPI (10 μM) and NOD-NPs (0.08 mg mL^{-1}) for 30 min successively, then irradiated with 365 nm light for 1 to 10 seconds. (b) The cells were incubated with DAPI and NOD-NPs as in the previous method, then exposed to 450 nm blue light for 30 to 60 seconds. Scale bar: 25 μm.

intracellular green fluorescence intensity was not further enhanced (Fig. 4A). Under this intensity of UV light, NO release is difficult to carry out in cells. The instantaneous reaction may be induced by the efficient absorption of UV light and the pervasive reducing substances in bio-systems.[30,44] Considering the unavoidable reducing agents in cells, choosing an appropriate wavelength for the excitation light is a possible solution. RAW 264.7 cells were treated with DAPI and NOD-NPs, then exposed to 450 nm blue light for 30 s. Fluorescence signals emerged around the cell nuclei. Upon irradiation of the cells for another 30 s, a great improvement in the green fluorescence was observed (Fig. 4B). Given the photo-toxicity induced by UV light, blue light would be more suitable for releasing NO in cells. Therefore, 450 nm light was engaged in activating the nanoparticles to release NO in the next biological experiments. The complete isolation of the blue and green fluorescence proved that NOD-NPs are non-invasive towards the nucleus.

To explore the improvement in biocompatibility upon forming the co-polymer NO donor, we used the CCK8 assay to compare the cytotoxicity of the NOD-NPs and NOD-C18. The cells were incubated with the NOD-NPs and monomer NOD-C18 for 48 h. As shown in Fig. 5, the viability of cells treated with NOD-NPs (0.08–0.64 mg mL^{-1}) decreased from 90% to 49%. And the IC_{50} value of NOD-NPs is calculated as 0.63 mg mL^{-1}. In sharp contrast, the corresponding content of NOD-C18 led to obvious cell death and the IC_{50} value of NOD-C18 is 1.48 μg mL^{-1}. Using the single molecular NO donor NOD-C18 would greatly inhibit the cell viability. The FDA approved lipidosome DSPE-PEG is widely applied to reduce biotoxicity in drug delivery. Reasonably, the results of cell viability certify that the formation of nanoparticles would significantly reduce the cytotoxicity, especially at a high concentration.

To further validate the biological safety of NOD-NPs, a hemolysis test with rat erythrocytes was performed. All animals received care according to the guidelines of the Care and Use of Laboratory Animals. The procedures were approved by the Guangxi University of Chinese Medicine Institutional Animal Welfare and Ethical Committee (DW20220617-226). The rat erythrocytes (2%) were treated with PBS and Triton X-100, and different concentrations of NOD-NPs. As a negative control, PBS did not affect hemolysis. Meanwhile the hemolysis rate with the positive control Triton X-100 was approximately 92%. With or without blue light irradiation, the NOD-NPs (0.013–0.1 mg mL^{-1}) generated a negligible increase in the hemolysis rate (Fig. S9†). The cell viability and hemolysis experiments clearly proved the good biocompatibility of our NO-releasing nanoparticles. Encouraged by the good intracellular applicability of NOD-NPs, we further evaluated their anti-bacterial effects on *E. coli* and *S. aureus*. The NOD-NPs (0.08 mg mL^{-1}) were loaded into the bacteria by co-incubation for 2 h. Then the residue was washed off, and the observation of NO release in bacteria was carried out using a confocal microscope. As shown in Fig. 6, no fluorescence was observed before exposure to light. Next, the bacteria were irradiated using 450 nm blue light (40 mW cm^{-2}) for 10 s to 30 s. A gradual enhancement of fluorescence emerged in *E. coli*, and the same phenomenon was noticed in *S. aureus*, which means controlled release of NO from NOD-NPs. Although NO is a potent anti-bacterial compound, all the bacteria exposed to this low concentration of NO remained in a regular morphology. We estimated that the NO released by our nanoparticles was ineffective at this concentration, since the dose is the crucial factor in anti-bacterial capacity.[45]

As a consequence, we raised the concentration of NOD-NPs (0.2, 0.4, and 0.8 mg mL^{-1}) to evaluate the antibacterial effect by a colony count test. First, we treated *E. coli* with PBS, Nap-C18, kanamycin, and NOD-NPs. Without light exposure, the antibiotic drug kanamycin killed all the bacteria, while the other treatments showed a negligible effect in suppressing the multiplication of *E. coli*. With 450 nm light irradiation, NOD-NPs showed dose-dependent anti-bacterial properties upon counting the total number of colonies on the culture plates. And the bacterial viability decreased from 63% to 6% (Fig. 7a). Since the nanoparticles and their decomposition product were ineffective against bacteria, we attributed the inhibition of *E. coli* to NO released by NOD-NPs. A parallel experiment was performed

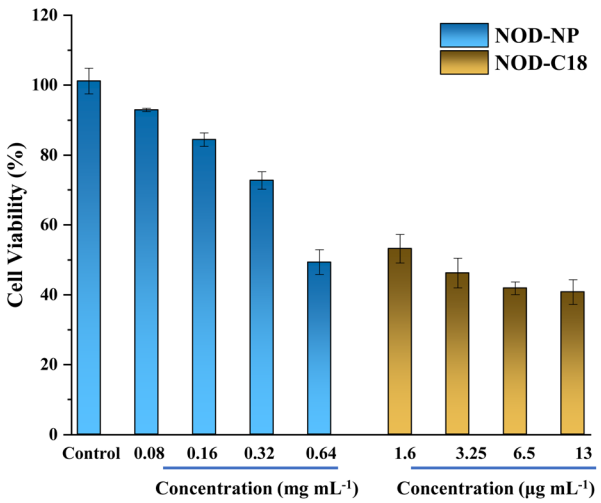

Fig. 5 The cell viabilities of NOD-NPs and NOD-C18 at various concentrations. 13 μg mL^{-1} NOD-C18 is encapsulated with 0.1 mg mL^{-1} NOD-NPs, and the other data are set similarly.

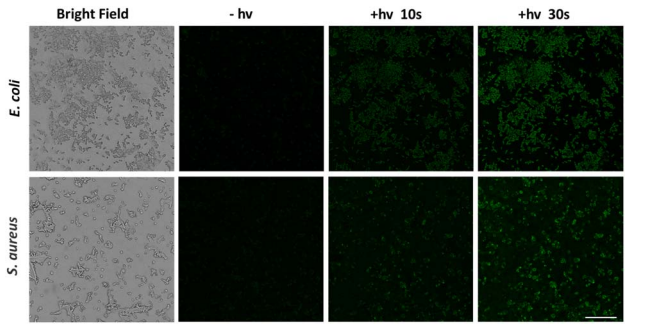

Fig. 6 The fluorescence images of *E. coli* and *S. aureus* bacteria imaged using a confocal laser scanning microscope. The bacteria were treated with NOD-NPs (0.08 mg mL^{-1}) for 2 h and then irradiated with 450 nm blue light for various times. Scale bar: 25 μm.

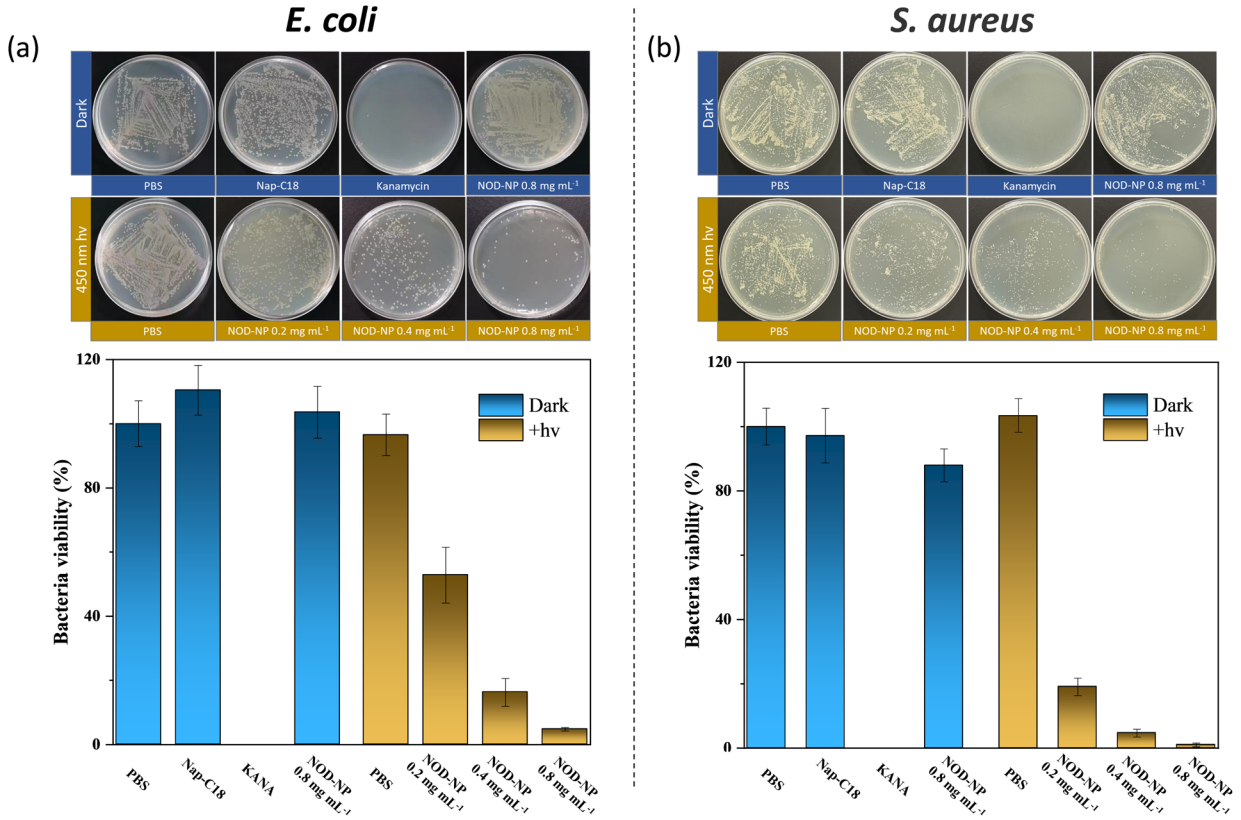

Fig. 7 The colony count test for (a) *E. coli* and (b) *S. aureus*. After treatment with different methods, the culture media of the bacteria were smeared on the plates and cultured for 24 h. KANA = kanamycin.

with *S. aureus*. As shown in Fig. 7b, a very similar outcome was observed for the two kinds of bacteria. The viability of *S. aureus* decreased to 3% after treatment with NO released by NOD-NPs. It was calculated that the minimum inhibitory concentration (MIC) against *E. coli* is 0.877 mg mL^{-1}, meanwhile the MIC value for *S. aureus* is 0.774 mg mL^{-1}. According to these results, we could determine that NOD-NPs are able to inhibit the proliferation of both *E. coli* and *S. aureus* by releasing NO.

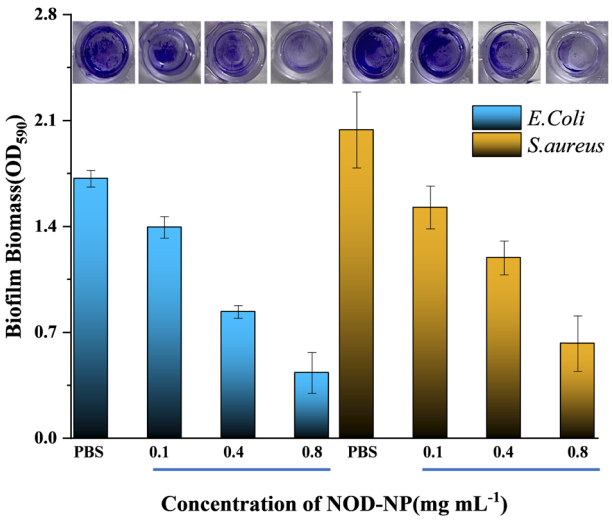

Fig. 8 Biofilm elimination experiments on *E. coli* and *S. aureus*. The biofilms were treated with different concentrations of NOD-NPs, and irradiated with 450 nm light (10 min at 10 mW cm^{-2}). Then the biofilm biomass was calculated using a crystal violet staining assay.

It is widely accepted that NO is a robust antibiofilm agent, which exhibits a synergistic anti-bacterial effect with antibiotics.[46,47] The anti-biofilm capacity of NOD-NPs was investigated *via* a crystal violet staining assay. The biofilms were treated with PBS or various doses of NOD-NPs, and then exposed to blue light (40 mW cm^{-2}) for 30 min. As depicted in Fig. 8, 0.1–0.8 mg mL^{-1} NOD-NPs reduced the biofilm biomass of *E. coli* by 17.7 to 71.1%. And the nanoparticles inhibited *S. aureus*' biofilm formation by 34.4 to 66.5%. The results suggested that NOD-NPs are effective in inhibiting biofilm formation. However, the biofilm inhibitory effect is not so evident. We speculated that the effect of separate use of NO to inhibit biofilms is limited, and the anti-biofilm capability of NO is mainly demonstrated *via* the synergistic effect with antibiotics.[48–50]

Conclusions

Herein, nanoparticles with excellent biocompatibility, NOD-NPs, were developed, and their photo-physical properties were evaluated in aqueous solution and cells. The NOD-NPs could release NO upon light irradiation, and spontaneously generate a green fluorescence signal. Moreover, the fluorescence

intensity was used to calibrate the flux of NO-release, without utilizing an additional analysis approach. The NO-release dynamics of NOD-NPs could be controlled not only by 365 nm UV light but also by 450 nm visible light. And the cell viability and hemolysis experiments proved that nanoparticle formation reduced the cytotoxicity. Since 450 nm light could control NO-release and was compatible with bio-systems, the antibacterial effect of NOD-NPs reached 94% in *E. coli* and 96% in *S. aureus*. And the biofilm dispersal caused by NOD-NPs was a decent result. Altogether, the NO-releasing nanoparticles are a convenient and safe tool for NO delivery in bio-systems, and an ideal candidate for evaluating the anti-bacterial effect of NO.

Conflicts of interest

There are no conflicts to declare.

Acknowledgements

This work is supported by the National Natural Science Foundation of China (No. 21908032), the Science and Technology Planning Project of Guangxi (2020AC19096), the Science and Technology Planning Project of Guangxi (AD20297005), the Initial Scientific Research Fund of Guangxi University of Chinese Medicine (2017BS043), and the Foundation of Guangxi Educational Committee (2022KY0308).

References

1 S. Ülker, D. McMaster, P. P. McKeown and U. Bayraktutan, *Cardiovasc. Res.*, 2003, **59**, 488–500.
2 H. Li, K. Witte, M. August, I. Brausch, U. Gödtel-Armbrust, A. Habermeier, E. I. Closs, M. Oelze, T. Münzel and U. Förstermann, *J. Am. Coll. Cardiol.*, 2006, **47**, 2536–2544.
3 L. Sun, W. Jiang, H. Zhang, Y. Guo, W. Chen, Y. Jin, H. Chen, K. Du, H. Dai, J. Ji and B. Wang, *ACS Appl. Mater. Interfaces*, 2019, **11**, 2302–2316.
4 R. F. Furchgott and J. V. Zawadzki, *Nature*, 1980, **288**, 373–376.
5 M. W. Radomski, R. M. Palmer and S. Moncada, *Br. J. Pharmacol.*, 1987, **92**, 639–646.
6 L. J. Ignarro, G. M. Buga, K. S. Wood, R. E. Byrns and G. Chaudhuri, *Proc. Natl. Acad. Sci. U. S. A.*, 1987, **84**, 9265–9269.
7 M. J. Joyner and N. M. Dietz, *J. Appl. Physiol.*, 1997, **83**, 1785–1796.
8 C. Napoli, G. Paolisso, A. Casamassimi, M. Al-Omran, M. Barbieri, L. Sommese, T. Infante and J. Ignarro Louis, *J. Am. Coll. Cardiol.*, 2013, **62**, 89–95.
9 S. R. Vincent, *Prog. Neurobiol.*, 2010, **90**, 246–255.
10 P. Crosswhite and Z. Sun, *J. Hypertens.*, 2010, **28**, 201–212.
11 J. B. Hibbs Jr., *J. Infect. Dis.*, 2002, **185**, S9–S17.
12 D. P. Arora, S. Hossain, Y. Xu and E. M. Boon, *Biochemistry*, 2015, **54**, 3717–3728.
13 D. A. Riccio and M. H. Schoenfisch, *Chem. Rev.*, 2012, **41**, 3731–3741.
14 J. A. Bauer, B. P. Booth and H.-L. Fung, *Adv. Pharmacol.*, 1995, **34**, 361–381.
15 P. G. Wang, M. Xian, X. Tang, X. Wu, Z. Wen, T. Cai and A. J. Janczuk, *Chem. Rev.*, 2002, **102**, 1091–1134.
16 D. Tsikas, *Free Radical Res.*, 2005, **39**, 797–815.
17 Q. Li and J. R. Lancaster, *Nitric Oxide*, 2009, **21**, 69–75.
18 P. R. Escamilla, Y. Shen, Q. Zhang, D. S. Hernandez, C. J. Howard, X. Qian, D. Y. Filonov, A. V. Kinev, J. B. Shear, E. V. Anslyn and Y. Yang, *Chem. Sci.*, 2020, **11**, 1394–1403.
19 L. E. McQuade and S. J. Lippard, *Curr. Opin. Chem. Biol.*, 2010, **14**, 43–49.
20 X. Zhang, J. Du, Z. Guo, J. Yu, Q. Gao, W. Yin, S. Zhu, Z. Gu and Y. Zhao, *Adv. Sci.*, 2019, **6**, 1801122.
21 Y. Chen, *Nitric Oxide*, 2020, **98**, 1–19.
22 C. M. Pavlos, H. Xu and J. P. Toscano, *Free Radical Biol. Med.*, 2004, **37**, 745–752.
23 S. Wecksler, A. Mikhailovsky and P. C. Ford, *J. Am. Chem. Soc.*, 2004, **126**, 13566–13567.
24 T. Suzuki, O. Nagae, Y. Kato, H. Nakagawa, K. Fukuhara and N. Miyata, *J. Am. Chem. Soc.*, 2005, **127**, 11720–11726.
25 A. P. Dicks, H. R. Swift, D. L. H. Williams, A. R. Butler, H. H. Al-Sa'doni and B. G. Cox, *J. Chem. Soc., Perkin Trans. 2*, 1996, **4**, 481–487.
26 F. Jia, Y. Deng and J. Ji, *Mater. Chem. Front.*, 2018, **2**, 830–834.
27 K. H. Cha, X. Wang and M. E. Meyerhoff, *Appl. Mater. Today*, 2017, **9**, 589–597.
28 Y. Wo, E. J. Brisbois, R. H. Bartlett and M. E. Meyerhoff, *Biomater. Sci.*, 2016, **4**, 1161–1183.
29 D. J. Suchyta, H. Handa and M. E. Meyerhoff, *Mol. Pharmaceutics*, 2014, **11**, 645–650.
30 Z. Zhang, J. Wu, Z. Shang, C. Wang, J. Cheng, X. Qian, Y. Xiao, Z. Xu and Y. Yang, *Anal. Chem.*, 2016, **88**, 7274–7280.
31 E. Y. Zhou, H. J. Knox, C. J. Reinhardt, G. Partipilo, M. J. Nilges and J. Chan, *J. Am. Chem. Soc.*, 2018, **140**, 11686–11697.
32 Z. Zhang, X. Luo and Y. Yang, *Isr. J. Chem.*, 2021, **61**, 159–168.
33 H. He, T. He, Z. Zhang, X. Xu, H. Yang, X. Qian and Y. Yang, *Chin. Chem. Lett.*, 2018, **29**, 1497–1499.
34 M. M. Lozano and M. L. Longo, *Langmuir*, 2009, **25**, 3705–3712.
35 S. Sriwongsitanont and M. Ueno, *Colloid Polym. Sci.*, 2004, **282**, 753–760.
36 J. Qi, L. Feng, X. Zhang, H. Zhang, L. Huang, Y. Zhou, Z. Zhao, X. Duan, F. Xu, R. T. K. Kwok, J. W. Y. Lam, D. Ding, X. Xue and B. Z. Tang, *Nat. Commun.*, 2021, **12**, 960.
37 H. Bian, D. Ma, X. Zhang, K. Xin, Y. Yang, X. Peng and Y. Xiao, *Small*, 2021, **17**, 2100398.
38 S. Qiu, C. Guo, M. Wang, Z. Sun, H. Li, X. Qian and Y. Yang, *Org. Chem. Front.*, 2018, **5**, 3206–3209.
39 H. He, Y. Liu, Z. Zhou, C. Guo, H.-Y. Wang, Z. Wang, X. Wang, Z. Zhang, F.-G. Wu, H. Wang, D. Chen, D. Yang, X. Liang, J. Chen, S. Zhou, X. Liang, X. Qian and Y. Yang, *Free Radical Biol. Med.*, 2018, **123**, 1–7.
40 N. Nakatsubo, H. Kojima, K. Sakurai, K. Kikuchi, H. Nagoshi, Y. Hirata, T. Akaike, H. Maeda, Y. Urano,

T. Higuchi and T. Nagano, *Biol. Pharm. Bull.*, 1998, **21**, 1247–1250.
41 L. Schmölz, M. Wallert and S. Lorkowski, *J. Immunol. Methods*, 2017, **449**, 68–70.
42 K. He, Z. Shen, Z. Chen, B. Zheng, S. Cheng and J. Hu, *Polym. Chem.*, 2021, **12**, 6344–6354.
43 Y. Opoku-Damoah, R. Zhang, H. T. Ta and Z. P. Xu, *Exploration*, 2022, 20210181.
44 X. Xu, M. Sun, X. Luo, Z. Zhang, L. Su, L. Cui, Z. Zhu, X. Lu, R. Wang, F. Han, X. Qian and Y. Yang, *Free Radical Biol. Med.*, 2021, **164**, 13–19.
45 F. Rong, Y. Tang, T. Wang, T. Feng, J. Song, P. Li and W. Huang, *Antioxidants*, 2019, **8**, 556.
46 H. Yu, S. Yu, H. Qiu, P. Gao, Y. Chen, X. Zhao, Q. Tu, M. Zhou, L. Cai, N. Huang, K. Xiong and Z. Yang, *Bioact. Mater.*, 2021, **6**, 1618–1627.
47 A. Mondal, P. Singha, M. Douglass, L. Estes, M. Garren, L. Griffin, A. Kumar and H. Handa, *ACS Appl. Mater. Interfaces*, 2021, **13**, 43892–43903.
48 H. Yu, L. X. Cui, N. Huang and Z. L. Yang, *Med. Gas Res.*, 2019, **9**, 184–191.
49 Z. Yuan, C. Lin, Y. He, B. Tao, M. Chen, J. Zhang, P. Liu and K. Cai, *ACS Nano*, 2020, **14**, 3546–3562.
50 Y.-T. Yu, S.-W. Shi, Y. Wang, Q.-L. Zhang, S.-H. Gao, S.-P. Yang and J.-G. Liu, *ACS Appl. Mater. Interfaces*, 2020, **12**, 312–321.